EMBO reports

scientific report

Ataxia telangiectasia mutated activation by transcription- and topoisomerase I-induced DNA double-strand breaks

Olivier Sordet[1†], Christophe E. Redon[1], Josée Guirouilh-Barbat[1], Susan Smith[2], Stéphanie Solier[1], Céline Douarre[1], Chiara Conti[1], Asako J. Nakamura[1], Benu B. Das[1], Estelle Nicolas[3], Kurt W. Kohn[1], William M. Bonner[1] & Yves Pommier[1+]

[1]Laboratory of Molecular Pharmacology, National Cancer Institute, NIH, and [2]Surgical Neurology Branch, National Institute of Neurological Disorders and Stroke, NIH, Bethesda, Maryland, USA, and [3]LBCMCP, UMR5088 CNRS, Université Paul Sabatier, Toulouse, France

Ataxia telangiectasia mutated (ATM), the deficiency of which causes a severe neurodegenerative disease, is a crucial mediator for the DNA damage response (DDR). As neurons have high rates of transcription that require topoisomerase I (TOP1), we investigated whether TOP1 cleavage complexes (TOP1cc)—which are potent transcription-blocking lesions—also produce transcription-dependent DNA double-strand breaks (DSBs) with ATM activation. We show the induction of DSBs and DDR activation in post-mitotic primary neurons and lymphocytes treated with camptothecin, with the induction of nuclear DDR foci containing activated ATM, γ-H2AX (phosphorylated histone H2AX), activated CHK2 (checkpoint kinase 2), MDC1 (mediator of DNA damage checkpoint 1) and 53BP1 (p53 binding protein 1). The DSB–ATM–DDR pathway was suppressed by inhibiting transcription and γ-H2AX signals were reduced by RNase H1 transfection, which removes transcription-mediated R-loops. Thus, we propose that Top1cc produce transcription arrests with R-loop formation and generate DSBs that activate ATM in post-mitotic cells.

Keywords: ATM; DNA double-strand break; R-loop; topoisomerase; transcription

EMBO reports (2009) **10,** 887–893. doi:10.1038/embor.2009.97

INTRODUCTION

DNA double-strand breaks (DSBs) are among the most severe genomic lesions and their repair requires the recruitment of DNA damage response (DDR) proteins (Bakkenist & Kastan, 2004; Shiloh, 2006). The loss of function of DDR proteins leads to Genomic instability and human hereditary diseases such as ataxia telangiectasia syndrome (AT caused by ataxia telangiectasia mutated (ATM) deficiency; Rass *et al*, 2007). The gene product of ATM is a serine/threonine protein kinase activated by DSBs (Bakkenist & Kastan, 2003). As AT is primarily a neurodegenerative disease and as neurons have high transcription rates, we examined whether transcription-blocking DNA lesions could induce DSBs and activate the ATM-associated DDR.

Topoisomerase I (TOP1) is required to remove DNA supercoiling generated by transcription. It relaxes supercoiling by producing transient TOP1 cleavage complexes (TOP1cc), which are TOP1-linked DNA single-strand breaks (Pommier, 2006). The rapid resealing of TOP1cc is inhibited by common DNA base alterations (oxidation, alkylation, base mismatch, base loss), carcinogenic adducts and DNA nicks (Pourquier & Pommier, 2001). TOP1cc can also be trapped selectively by the plant alkaloid camptothecin (CPT), the semi-synthetic derivatives of which, topotecan and irinotecan, are used to treat human cancers (Pommier, 2006). Trapped TOP1cc are potent transcription-blocking DNA lesions (Ljungman & Lane, 2004; Capranico *et al*, 2007). Transcription complexes might be blocked physically a few base pairs upstream of the TOP1cc and their progression arrested by the accumulation of positive DNA supercoiling ahead of the transcribing RNA polymerase II (Pol II; Capranico *et al*, 2007).

Owing to the high rate of oxygen consumption, neurons produce reactive oxygen species that can damage DNA and trap TOP1cc (Pourquier & Pommier, 2001; Daroui *et al*, 2004; Pommier, 2006). In agreement with this possibility, defective repair of TOP1cc (by inactivating mutation of tyrosyl-DNA-phosphodiesterase 1 (TDP1)) leads to the hereditary spinocerebellar ataxia with axonal neuropathy (SCAN) syndrome (Rass *et al*, 2007). Here, we used CPT to induce TOP1cc in non-replicating cells to determine whether transcription-blocking TOP1cc induce DSBs and activate the ATM-associated DDR.

[1]Laboratory of Molecular Pharmacology, National Cancer Institute, Building 37, Room 5068, NIH, Bethesda, MD 20892-4255, USA
[2]Surgical Neurology Branch, National Institute of Neurological Disorders and Stroke, NIH, Bethesda, MD 20892, USA
[3]LBCMCP, UMR5088 CNRS, Université Paul Sabatier, 31062 Toulouse, France
[†]Present address: INSERM U563, Institut Claudius Regaud, 31052 Toulouse, France
[+]Corresponding author. Tel: +1 301 496 5944; Fax: +1 301 402 0752;
E-mail: pommier@nih.gov

Received 6 January 2009; revised 30 March 2009; accepted 9 April 2009; published online 26 June 2009

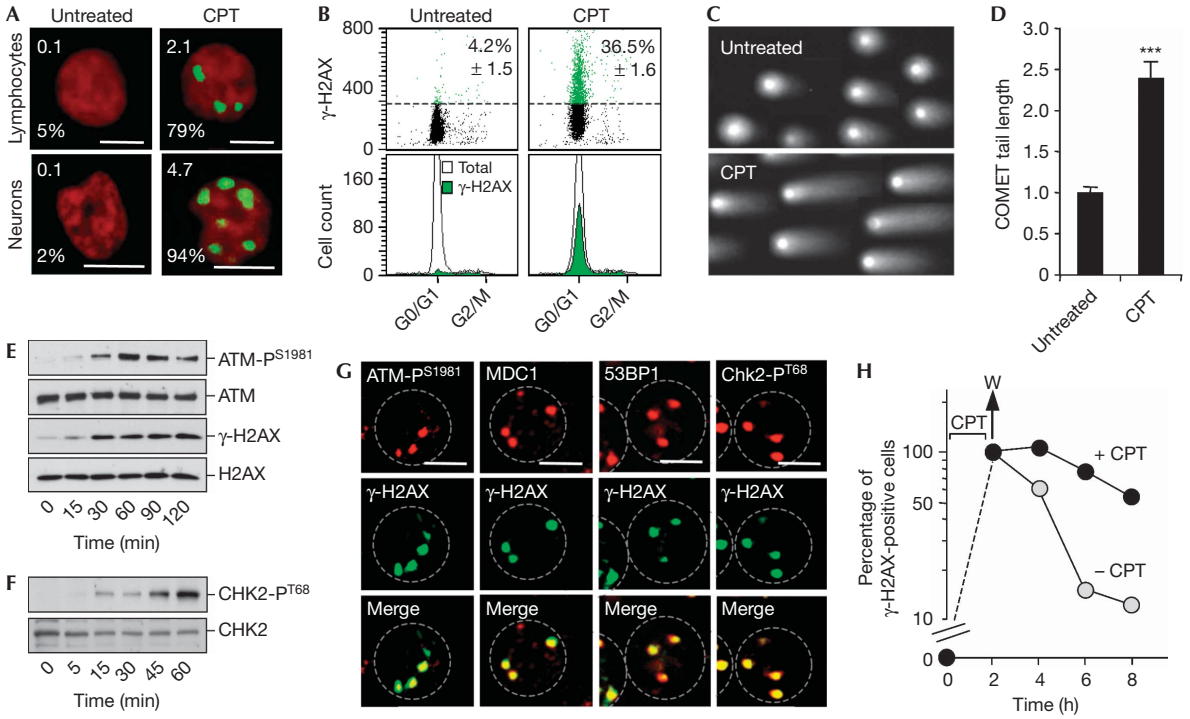

Fig 1 | Induction of DNA double-strand breaks and activation of the ataxia telangiectasia mutated pathway in post-mitotic cells in response to camptothecin. (**A**) γ-H2AX foci in human lymphocytes and rat cortical neurons treated with 25 μM CPT for 1 h before staining for γ-H2AX (green). DNA was counterstained with propidium iodide (red). Numbers indicate the percentage of cells with at least one γ-H2AX focus (bottom) and the average number of γ-H2AX foci per cell (top). Scale bar, 5 μm. (**B**) Flow cytometry analysis of γ-H2AX and DNA contents (PI staining) in human lymphocytes treated with 25 μM CPT for 2 h. Top panels: numbers are the percentage of γ-H2AX-positive cells (average ± standard deviation), which are coloured in green. Bottom panels: a comparison of the γ-H2AX-positive fraction (green) with the total DNA content of the population (white). (**C,D**) Induction of double-strand breaks in rat neurons. Cells were treated with 25 μM CPT for 1 h and DSBs were detected by neutral COMET assay. (**C**) Representative pictures of nuclei. (**D**) Quantification of the COMET tail length (average ± standard deviation, 30–40 cells were examined per group). Asterisks denote significant difference from untreated cells ($P<0.001$; *t*-test). (**E,F**) Phosphorylation of ATM on Ser 1981 (ATM-P^{S1981}), H2AX on Ser 139 (γ-H2AX) and CHK2 on Thr 68 (CHK2-P^{T68}) was determined by Western blotting in human lymphocytes treated with 25 μM CPT. Total ATM, H2AX and CHK2 were examined in parallel. (**G**) Colocalization of γ-H2AX foci with ATM-P^{S1981}, MDC1, 53BP1 and CHK2-P^{T68}. Human lymphocytes were treated with 25 μM CPT for 1 h before staining. Images were merged to determine colocalization (yellow). Scale bar, 5 μm. Nuclear outlines are shown. (**H**) Reversal of γ-H2AX after CPT removal. Human lymphocytes were treated with 25 μM CPT for 2 h, and washed (W) and cultured in CPT-free medium (−CPT) for the indicated times. Unwashed cells (+CPT) were examined in parallel. Percentages of γ-H2AX-positive cells were determined by flow cytometry as described in (**B**) and normalized to the level at the time of CPT removal, which was taken at 100%. ATM, ataxia telangiectasia mutated; 53BP1, p53 binding protein 1; CHK2, checkpoint kinase 2; CPT, camptothecin; DSBs, double-strand breaks; γ-H2AX, phosphorylated histone H2AX; MDC1, mediator of DNA damage checkpoint 1; PI, propidium iodide.

RESULTS AND DISCUSSION

DNA breaks and ATM activation in post-mitotic cells

To determine whether TOP1cc can induce DDR in post-mitotic cells, we examined the phosphorylated histone H2AX at Ser 139 (γ-H2AX) and its accumulation in nuclear foci. A single γ-H2AX focus reflects hundreds to thousands of γ-H2AX proteins that are concentrated around at least one DSB (Bonner *et al*, 2008). In primary human lymphocytes and rat cortical neurons, CPT induced γ-H2AX foci within 1 h, with an average of approximately 2 and 5 γ-H2AX foci per nucleus, respectively (Fig 1A). Most cells formed at least one γ-H2AX focus (79% of lymphocytes and 94% of neurons; Fig 1A; supplementary Fig S1A,B online). Flow cytometry, albeit not as sensitive as microscopy, confirmed γ-H2AX induction in non-replicating cells (Fig 1B) and neutral COMET assays showed the presence of DSBs (Fig 1C,D). These results indicate the induction of replication-independent DSBs by TOP1cc in post-mitotic cells, aside from the well-established replication-associated DSBs in proliferating cells (Furuta *et al*, 2003).

Next, we examined the response of post-mitotic cells to DSBs induced by TOP1cc by investigating the activation of DDR proteins and their recruitment to the γ-H2AX foci. DSBs rapidly activate ATM, which phosphorylates checkpoint kinase 2 (CHK2), mediator of DNA damage checkpoint 1 (MDC1), p53 binding protein 1 (53BP1) and H2AX at damaged sites (Bakkenist & Kastan, 2004; Shiloh, 2006). In primary lymphocytes, CPT induced rapid ATM autophosphorylation at Ser 1981 (ATM-PS1981; Fig 1E), which reflects ATM activation (Bakkenist & Kastan, 2003). ATM-PS1981 colocalized with the γ-H2AX foci (Fig 1G) together with activated CHK2 (phosphorylated at Thr 68; Fig 1F,G; supplementary Fig S2 online),

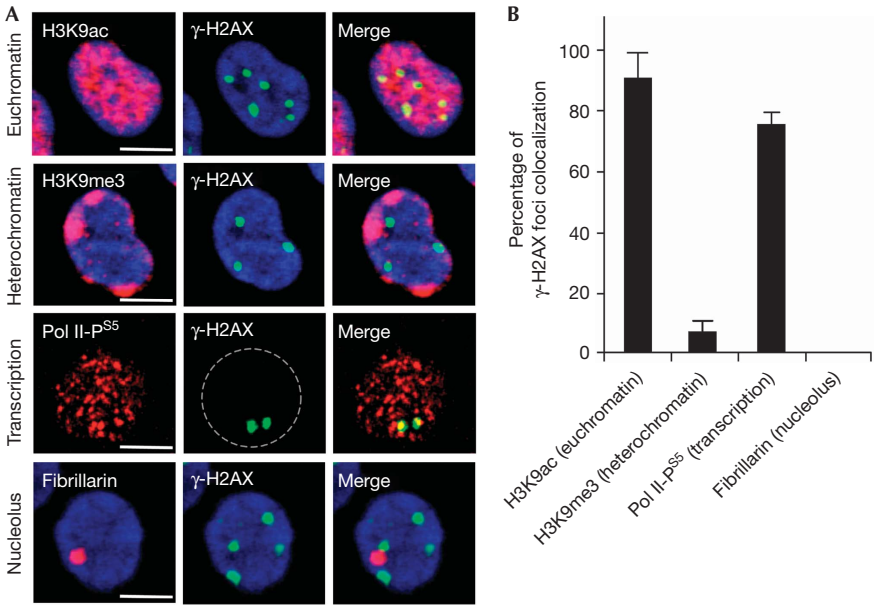

Fig 2 | γ-H2AX foci colocalize with transcribed regions in post-mitotic cells treated with camptothecin. (**A**) Human lymphocytes were treated with 25 μM CPT for 1 h before staining for γ-H2AX (green), and H3K9ac (euchromatin marker; red), H3K9me3 (heterochromatin marker; red), fibrillarin (nucleolus marker; red) or Pol II phosphorylated on Ser 5 (Pol II-P^{S5}, transcription marker; red). Images were merged to determine colocalization (yellow). DNA was counterstained with DAPI (blue). Bars correspond to 5 μM. (**B**) Percentages of γ-H2AX foci colocalizing with H3K9ac, H3K9me3, fibrillarin or Pol II-P^{S5} in lymphocytes treated as in (**A**). Three hundred γ-H2AX foci were analysed in each group (average ± standard deviation). CPT, camptothecin; DAPI, 4′,6-diamidino-2-phenylindole; γ-H2AX, phosphorylated histone H2AX; H3K9ac, acetylation of histone H3 on lysine 9; H3K9me3, trimethylation of H3K9.

MDC1 and 53BP1 (Fig 1G). However, these DDR foci did not colocalize with promyelocytic leukaemia (PML) bodies (supplementary Fig S1C–E online). Fig 1H shows the reversibility of γ-H2AX, which is consistent with the repair of the TOP1-induced DNA lesions on CPT removal (Pommier, 2006). Taken together, the above experiments indicate that the induction of DSBs by TOP1cc reversibly activates the ATM-associated DDR pathway in non-replicating cells.

Transcription-induced DNA breaks and ATM activation

The replication-independent γ-H2AX foci induced by CPT formed in euchromatin regions and were excluded from heterochromatin, in which genes are silenced (Fig 2). They were also excluded from nucleoli and coincided with sites in which Pol II was hyperphosphorylated at Ser 5 (Fig 2), suggesting the formation of γ-H2AX foci at sites where transcribing Pol II is arrested by TOP1cc (Sordet *et al*, 2008).

Further evidence that DSB induction and DDR activation were transcription-dependent was provided by the fact that inhibition of Pol II by 5,6-dichlorobenzimidazole 1-β-D-ribofuranoside (DRB), flavopiridol (FLV) and α-amanitin prevented CPT-induced γ-H2AX both in primary lymphocytes (Fig 3A,B; supplementary Fig S3A online) and in primary neurons (Fig 3C,D; supplementary Fig S3B online). Consistent with the γ-H2AX results, COMET assays showed DSB suppression by FLV (Fig 3E,F). FLV also reduced CPT-induced ATM autophosphorylation both in primary neurons (Fig 3G,D) and in lymphocytes (Fig 3H). The suppressive effect of FLV was not due to a reduction in CPT-induced TOP1cc (supplementary Fig S3E online) and was observed over a range of CPT concentrations (supplementary Fig S3B–D online). Thus, it is unlikely that the transcription-induced DSBs simply resulted from two nearby TOP1cc-associated single-strand breaks on opposing DNA strands. The fact that DRB, FLV and α-amanitin failed to induce DSBs, γ-H2AX and ATM by themselves (Fig 3) argues that CPT-induced DDR activation is induced by TOP1cc rather than transcription elongation arrest. Thus, we conclude that blocking Pol II by TOP1cc induces the formation of DSBs and activates DDR.

While our study was under review, Lin *et al* (2008) reported that CPT also induces transcription-dependent activation of ATM in serum-starved quiescent WI-38 fibroblasts. However, ATM activation was attributed to TOP1cc instead of DSBs based on the weak detection of γ-H2AX by Western blotting and a lack of neutral COMET tails. It is likely that the number of DSBs in quiescent WI-38 fibroblasts was close to or below the thresholds of detection of the Western blot assays used by the authors. Immunofluorescence microscopy for γ-H2AX is more sensitive than Western blotting as it can detect a single DSB focus per cell (Bonner *et al*, 2008). In fact, another paper published during the review of our study is consistent with our results, as it shows the induction of well-defined γ-H2AX foci in post-mitotic neurons treated with CPT (Tian *et al*, 2009).

R-loops (RNA–DNA hybrids) are known to induce DSBs and genomic instability (Li & Manley, 2005). R-loops result from the extended pairing of nascent messenger RNA (mRNA) with the corresponding unwound DNA template behind the elongating Pol II (Huertas & Aguilera, 2003). To determine the potential role of R-loops in TOP1cc-mediated DSBs, we tested whether

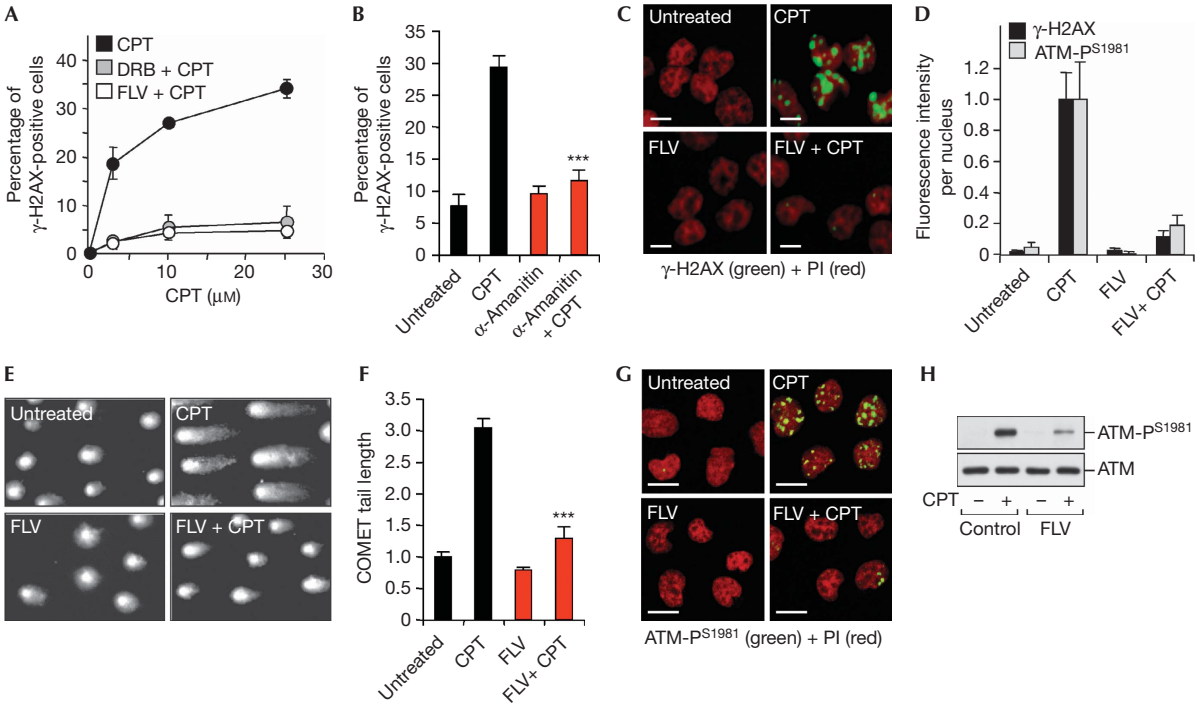

Fig 3 | Transcription-induced DNA double-strand breaks and ataxia telangiectasia mutated activation in post-mitotic cells in response to topoisomerase 1 cleavage complexes. (**A**,**B**) Inhibition of CPT-induced γ-H2AX by transcription inhibitors in human lymphocytes. Cells were treated for (**A**) 1 h with DRB (100 μM) or FLV (1 μM) or (**B**) for 17 h with α-amanitin (10 μM) before the addition of CPT (2 h with the indicated concentrations in (**A**); 2 h with 25 μM in (**B**). The percentage of γ-H2AX-positive cells (average ± standard deviation) were determined by flow cytometry as described in Fig 1B. Asterisks in (**B**) denote significant difference from CPT-treated cells in the absence of α-amanitin ($P<0.001$; *t*-test). (**C**) FLV prevents CPT-induced γ-H2AX foci in rat neurons. Cells were treated with FLV (1 μM, 1 h) before the addition of CPT (25 μM, 1 h) and then stained for γ-H2AX (green). DNA was counterstained with PI (red). Scale bar, 5 μm. (**D**) Quantification of γ-H2AX and ATM-P^{S1981} signal intensity per nucleus (average ± standard deviation) in rat cortical neurons treated as described in (**C**) and (**G**). (**E**,**F**) FLV prevents CPT-induced DSBs in rat neurons. Cells were treated with FLV (1 μM, 1 h) before the addition of CPT (25 μM, 1 h) and DSBs were detected by neutral COMET assay. (**E**) Representative picture of nuclei. (**F**) Quantification of the COMET tail length (average ± standard deviation, 30–40 cells were examined per group). Asterisks denote significant difference from CPT-treated cells in the absence of FLV ($P<0.001$; *t*-test). (**G**) FLV prevents CPT-induced ATM-P^{S1981} in rat neurons. Cells were treated with FLV (1 μM, 1 h) before the addition of CPT (25 μM, 1 h) and then stained for ATM-P^{S1981} (green). DNA was counterstained with PI (red). Scale bar, 5 μm. (**H**) FLV prevents CPT-induced ATM-P^{S1981} in human lymphocytes. Western blotting of ATM-P^{S1981} and total ATM in cells treated with FLV (1 μM, 1 h) before the addition of CPT (25 μM, 1 h). ATM, ataxia telangiectasia mutated; ATM-P^{S1981}, phosphorylation of ATM on Ser 1981; CPT, camptothecin; DRB, 5,6-dichlorobenzimidazole 1-β-D-ribofuranoside; DSBs, double-strand breaks; FLV, flavopiridol; γ-H2AX, phosphorylated histone H2AX; PI, propidium iodide.

overexpression of RNase H1, which degrades RNA in RNA–DNA hybrids, could prevent CPT-induced γ-H2AX. Fig 4 shows that overexpression of RNase H1 in post-mitotic primary neurons decreased the induction of γ-H2AX. Similar results were obtained in HeLa cells in which replication was blocked by aphidicolin before the addition of CPT (supplementary Fig S4 online). Thus, we propose that R-loops generated by stalled TOP1cc induce the formation of DSBs. R-loops might form as negative supercoiling accumulates behind the transcription complexes arrested by TOP1cc (Drolet *et al*, 2003). Inhibition of the SR-kinase activity of TOP1 by CPT (Soret *et al*, 2003) might also promote R-loops by interfering with splicing (Li & Manley, 2005).

ATM transduces transcription-induced DNA breaks

H2AX, similar to many other ATM substrates, can also be phosphorylated by DNA-dependent protein kinase (DNA-PK; Stiff *et al*, 2004) and ataxia telangiectasia and Rad3 related (ATR; Matsuoka *et al*, 2007). Although ATR can facilitate ATM activation (Stiff *et al*, 2006), it is unlikely to be involved here as ATR is suppressed in post-mitotic lymphocytes (Fig 5C; Jones *et al*, 2004). Thus, we focused on ATM and DNA-PK as candidate kinases for H2AX phosphorylation (Bonner *et al*, 2008). Pre-treatment of primary lymphocytes with the ATM kinase inhibitor KU55933 suppressed CPT-induced γ-H2AX (Fig 5A) under conditions in which ATM autophosphorylation was suppressed (Fig 5B). Similar results were obtained in primary neurons (Fig 5C; supplementary Fig S5 online). By contrast, the DNA-PK kinase inhibitor KU57788 did not affect CPT-induced γ-H2AX (Fig 5A). ATM kinase inhibition also suppressed the formation of CHK2-PT68 (Fig 5D) and 53BP1 nuclear foci (Fig 5E). As ATM can activate DNA-PK (Chen *et al*, 2007), we examined CPT-induced DNA-PK phosphorylation in post-mitotic cells and found DNA-PK phosphorylation at Ser 2056 and Thr 2609 (Fig 5B). Inhibition of DNA-PK or ATM prevented DNA-PK phosphorylation; by contrast,

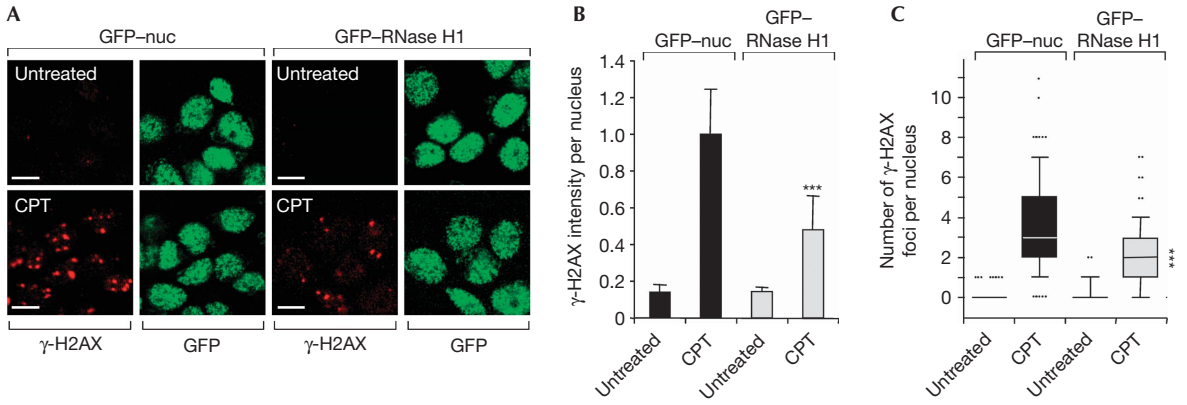

Fig 4 | Overexpression of RNase H1 decreases the induction of phosphorylated H2AX in post-mitotic cells in response to topoisomerase 1 cleavage complexes. (**A–C**) Rat neurons transfected with GFP–RNase H1 or with GFP alone containing nuclear targeting sequences (GFP–nuc) were treated with CPT (10 μM, 1 h) before staining for γ-H2AX (red) and GFP (green). (**A**) Representative pictures. Scale bar, 5 μm. (**B**) Quantification of γ-H2AX signal intensity per nucleus (average ± standard deviation). (**C**) Number of γ-H2AX foci per nucleus (130 nuclei were analysed). Boxes: 25–75 percentile range; whiskers: 10–90 percentile range; horizontal bars: median number of γ-H2AX foci. Each dot indicates an individual nucleus that is not in the 10–90 percentile range. Asterisks in (**B**) and (**C**) denote significant difference from CPT-treated GFP–nuc transfected cells ($P<0.001$; *t*-test). CPT, camptothecin; GFP, green fluorescent protein; γ-H2AX, phosphorylated histone H2AX.

inhibition of DNA-PK did not affect ATM autophosphorylation (Fig 5B). These results suggest that ATM promotes DNA-PK autophosphorylation and thereby its activation in post-mitotic cells. Although the DNA-PK-dependent non-homologous end-joining pathway is involved in the repair of DSBs in G0/G1 (Lieber *et al*, 2003), DNA-PK inhibition did not prevent the reversal of γ-H2AX on CPT removal in primary lymphocytes (data not shown), suggesting that other pathways are involved in repairing the transcription-associated DSBs in post-mitotic cells. Taken together, our findings indicate that ATM is the main transducer of the transcription-associated DSB response to TOP1cc in post-mitotic cells.

Speculation

We propose that transcription arrest by stalled TOP1cc generates R-loops that induce DSBs with activation of the DDR–ATM–CHK2 pathway (Fig 5F). These transcription- and TOP1cc-dependent DSBs, which are potentially lethal if not repaired, might contribute to the cytotoxicity of TOP1cc in post-mitotic neurons (Morris & Geller, 1996; Tian *et al*, 2009). ATM might prevent cumulative DNA lesions by quenching reactive oxygen species (Ito *et al*, 2004) and/or by inhibiting transcription (Kruhlak *et al*, 2007). Although ATM also signals DSB repair (Shiloh, 2006), it has been shown to preferentially repair DSBs associated with heterochromatin (Goodarzi *et al*, 2008), whereas transcription-mediated DSBs form in euchromatin (Fig 2). Besides its protective role, ATM can also promote cell-cycle re-entry of post-mitotic neurons, leading to neuronal death (Kruman *et al*, 2004; Tian *et al*, 2009). Transcription-mediated DSBs might occur spontaneously in normal neurons as TOP1cc are stabilized by endogenous oxidative DNA alterations (Pourquier & Pommier, 2001; Daroui *et al*, 2004). Hence, our findings suggest that the defective response to DSBs produced by TOP1cc might contribute to the neurodegenerative phenotype of AT patients (Rass *et al*, 2007). The endogenous DNA alterations leading to TOP1cc-dependent DSBs might occur at very low frequencies, as transcription-dependent DSBs were not detectable in response to exogenous oxidative stress (supplementary Fig S6 online), which might explain why the neurological defects of AT patients become prevalent after early childhood (Rass *et al*, 2007). Similarly, the neurodegenerative SCAN syndrome, which is related to the defective repair of TOP1cc, is detected late in the teenage years (Rass *et al*, 2007).

METHODS

Cell culture. Human peripheral lymphocytes were obtained from the Blood Bank at the NIH and maintained in RPMI 1640 medium supplemented with 10% fetal calf serum. Primary cortical neurons were prepared from embryonic day 18 rat fetuses, as described in the supplementary information online, and maintained in Neurobasal medium supplemented with 1:50 B27 and 1 mM L-glutamine.

Immunofluorescence confocal microscopy. Cytospins of human lymphocytes and cultures of rat cortical neurons were processed for immunofluorescence microscopy as described in the supplementary information online.

Flow cytometry analyses of γ-H2AX. Human lymphocytes were processed for flow cytometry as described in the supplementary information online using the anti-γ-H2AX antibody from Abcam (ab18311).

Neutral COMET assays. Neutral COMET assays in rat cortical neurons were performed according to the manufacturer's instructions (Trevigen, Gaithesburg, MD, USA), except that the electrophoresis was performed at 4 °C.

RNase H1 transfections. Rat cortical neurons were transfected with GFP–RNase H1 (a kind gift from Dr Crouch, NIH, Bethesda, MD, USA) or GPF–nuc (Invitrogen, Carlsbad, CA, USA) using NeuroPORTER (Sigma, St Louis, MO, USA) according to the manufacturer's protocol. Experiments were carried out 72 h after transfection.

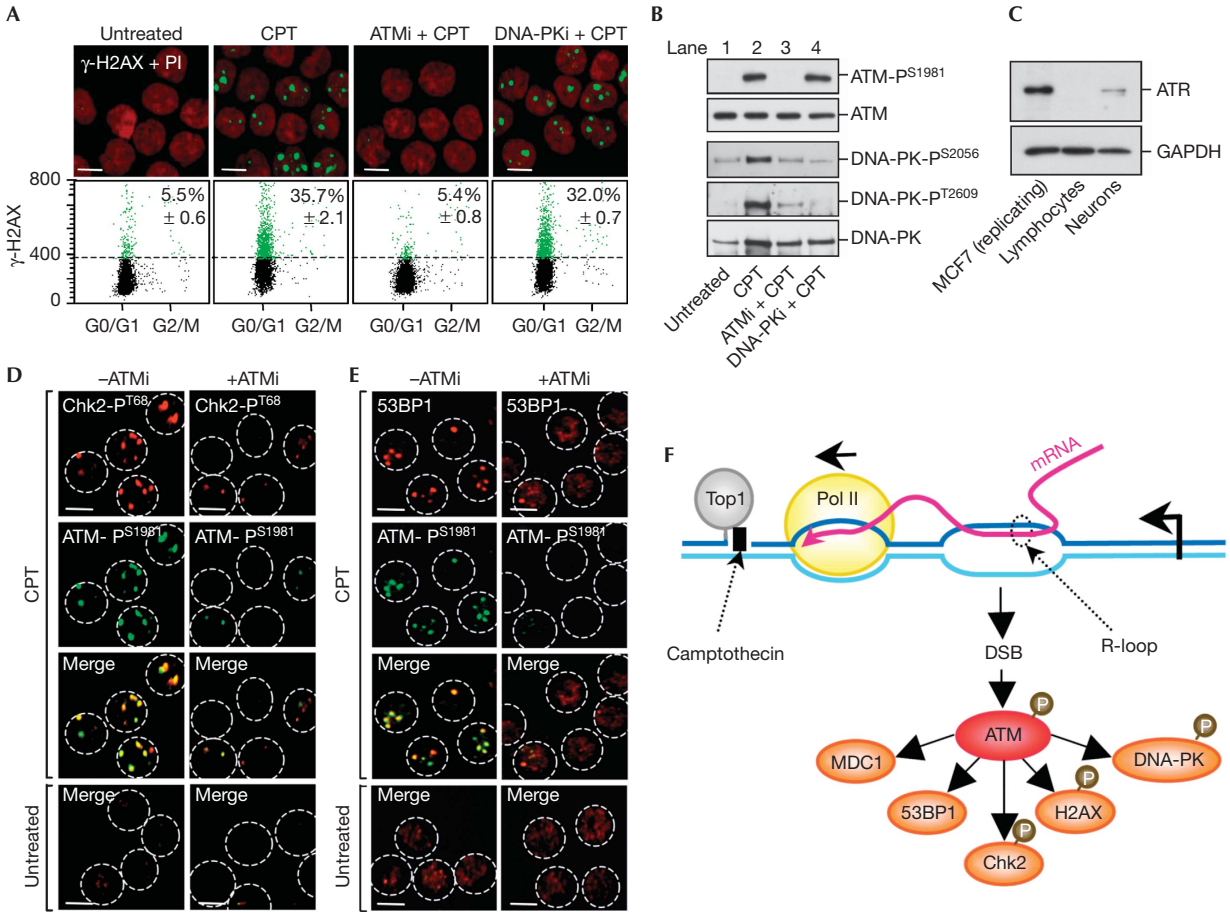

Fig 5 | Camptothecin-induced DNA damage response is ataxia telangiectasia mutated dependent in post-mitotic cells. (**A**) Inhibition of ATM prevents CPT-induced γ-H2AX in human lymphocytes. Cells were treated with the ATM kinase inhibitor KU55933 (ATMi, 10 μM) or the DNA-PK kinase inhibitor KU57788 (DNA-PKi, 10 μM) for 1 h before the addition of 25 μM CPT for 2 h. Top panels: cells were stained with γ-H2AX (green) and DNA was counterstained with PI (red). Scale bar, 5 μm. Bottom panels: flow cytometry analysis of γ-H2AX and DNA content (PI staining). Numbers indicate percentages of γ-H2AX-positive cells (average ± standard deviation), which are coloured in green. (**B**) Inhibition of ATM kinase prevents CPT-induced DNA-PK phosphorylation in human lymphocytes. Western blotting of ATM-P^{S1981}, DNA-PK-P^{S2056} and DNA-PK-P^{T2609}, ATM and DNA-PK in cells treated with ATMi or DNA-PKi as described in (**A**) before the addition of 25 μM CPT for 1 h. (**C**) Western blotting of ATR in human lymphocytes and rat neurons. The breast cancer MCF7 cells were used as a positive control for ATR expression; GAPDH was used as a loading control. (**D**,**E**) ATM inhibition prevents CPT-induced CHK2-P^{T68} and 53BP1 foci formation in human lymphocytes. Cells were treated with ATMi as described in (**A**) before the addition of 25 μM CPT for 1 h. Cells were then stained for (**D**) ATM-P^{S1981} (green) and CHK2-P^{T68} (red) or (**E**) for ATM-P^{S1981} (green) and 53BP1 (red). Nuclear outlines are highlighted. Scale bar, 5 μm. (**F**) Model for the induction of DSBs and the ATM pathway by TOP1cc-mediated transcription block. Stabilization of a TOP1cc by CPT interferes with transcription elongation and generates a hybrid RNA–DNA (R-loop). This promotes the induction of a DSB, which leads to autophosphorylation/activation of ATM in the vicinity of the DSB. ATM is activated upstream of DNA-PK and activates its substrates H2AX, CHK2, MDC1 and 53BP1 at the DSB site. ATM, ataxia telangiectasia mutated; ATR, ataxia telangiectasia and Rad3 related; 53BP1, p53 binding protein 1; CHK2, checkpoint kinase 2; CPT, camptothecin; DNA-PK, DNA-dependent protein kinase; DSB, double-strand break; GAPDH, glyceraldehyde-3-phosphate dehydrogenase; γ-H2AX, phosphorylated histone H2AX; MDC1, mediator of DNA damage checkpoint 1; PI, propidium iodide; TOP1cc, topoisomerase I cleavage complex.

Other materials and procedures are described in the supplementary information online.

Supplementary information is available at *EMBO reports* online (http://www.emboreports.org).

ACKNOWLEDGEMENTS

This research was supported by the Intramural Research Program of the National Institutes of Health, National Cancer Institute, Center for Cancer Research.

CONFLICT OF INTEREST

The authors declare that they have no conflict of interest.

REFERENCES

Bakkenist CJ, Kastan MB (2003) DNA damage activates ATM through intermolecular autophosphorylation and dimer dissociation. *Nature* **421:** 499–506

Bakkenist CJ, Kastan MB (2004) Initiating cellular stress responses. *Cell* **118:** 9–17

Bonner WM, Redon CE, Dickey JS, Nakamura AJ, Sedelnikova OA, Solier S, Pommier Y (2008) γ-H2AX and cancer. *Nat Rev Cancer* **8:** 957–967

Capranico G, Ferri F, Fogli MV, Russo A, Lotito L, Baranello L (2007) The effects of camptothecin on RNA polymerase II transcription: roles of DNA topoisomerase I. *Biochimie* **89:** 482–489

Chen BP, Uematsu N, Kobayashi J, Lerenthal Y, Krempler A, Yajima H, Lobrich M, Shiloh Y, Chen DJ (2007) Ataxia telangiectasia mutated (ATM) is essential for DNA-PKcs phosphorylations at the Thr 2609 cluster upon DNA double strand break. *J Biol Chem* **282:** 6582–6587

Daroui P, Desai SD, Li TK, Liu AA, Liu LF (2004) Hydrogen peroxide induces topoisomerase I-mediated DNA damage and cell death. *J Biol Chem* **279:** 14587–14594

Drolet M, Broccoli S, Rallu F, Hraiky C, Fortin C, Masse E, Baaklini I (2003) The problem of hypernegative supercoiling and R-loop formation in transcription. *Front Biosci* **8:** d210–d221

Furuta T *et al* (2003) Phosphorylation of histone H2AX and activation of Mre11, Rad50, and Nbs1 in response to replication-dependent DNA double-strand breaks induced by mammalian DNA topoisomerase I cleavage complexes. *J Biol Chem* **278:** 20303–20312

Goodarzi AA, Noon AT, Deckbar D, Ziv Y, Shiloh Y, Lobrich M, Jeggo PA (2008) ATM signaling facilitates repair of DNA double-strand breaks associated with heterochromatin. *Mol Cell* **31:** 167–177

Huertas P, Aguilera A (2003) Cotranscriptionally formed DNA:RNA hybrids mediate transcription elongation impairment and transcription-associated recombination. *Mol cell* **12:** 711–721

Ito K *et al* (2004) Regulation of oxidative stress by ATM is required for self-renewal of haematopoietic stem cells. *Nature* **431:** 997–1002

Jones GG, Reaper PM, Pettitt AR, Sherrington PD (2004) The ATR-p53 pathway is suppressed in noncycling normal and malignant lymphocytes. *Oncogene* **23:** 1911–1921

Kruhlak M, Crouch EE, Orlov M, Montano C, Gorski SA, Nussenzweig A, Misteli T, Phair RD, Casellas R (2007) The ATM repair pathway inhibits RNA polymerase I transcription in response to chromosome breaks. *Nature* **447:** 730–734

Kruman II, Wersto RP, Cardozo-Pelaez F, Smilenov L, Chan SL, Chrest FJ, Emokpae R Jr, Gorospe M, Mattson MP (2004) Cell cycle activation linked to neuronal cell death initiated by DNA damage. *Neuron* **41:** 549–561

Li X, Manley JL (2005) Inactivation of the SR protein splicing factor ASF/SF2 results in genomic instability. *Cell* **122:** 365–378

Lieber MR, Ma Y, Pannicke U, Schwarz K (2003) Mechanism and regulation of human non-homologous DNA end-joining. *Nat Rev Mol Cell Biol* **4:** 712–720

Lin CP, Ban Y, Lyu YL, Desai SD, Liu LF (2008) A ubiquitin-proteasome pathway for the repair of topoisomerase I-DNA covalent complexes. *J Biol Chem* **283:** 21074–21083

Ljungman M, Lane DP (2004) Transcription—guarding the genome by sensing DNA damage. *Nat Rev Cancer* **4:** 727–737

Matsuoka S *et al* (2007) ATM and ATR substrate analysis reveals extensive protein networks responsive to DNA damage. *Science* **316:** 1160–1166

Morris EJ, Geller HM (1996) Induction of neuronal apoptosis by camptothecin, an inhibitor of DNA topoisomerase-I: evidence for cell cycle-independent toxicity. *J Cell Biol* **134:** 757–770

Pommier Y (2006) Topoisomerase I inhibitors: camptothecins and beyond. *Nat Rev Cancer* **6:** 789–802

Pourquier P, Pommier Y (2001) Topoisomerase I-mediated DNA damage. *Adv Cancer Res* **80:** 189–216

Rass U, Ahel I, West SC (2007) Defective DNA repair and neurodegenerative disease. *Cell* **130:** 991–1004

Shiloh Y (2006) The ATM-mediated DNA-damage response: taking shape. *Trends Biochem Sci* **31:** 402–410

Sordet O, Larochelle S, Nicolas E, Stevens EV, Zhang C, Shokat KM, Fisher RP, Pommier Y (2008) Hyperphosphorylation of RNA polymerase II in response to topoisomerase I cleavage complexes and its association with transcription-and BRCA1-dependent degradation of topoisomerase I. *J Mol Biol* **381:** 540–549

Soret J, Gabut M, Dupon C, Kohlhagen G, Stevenin J, Pommier Y, Tazi J (2003) Altered serine/arginine-rich protein phosphorylation and exonic enhancer-dependent splicing in mammalian cells lacking topoisomerase I. *Cancer Res* **63:** 8203–8211

Stiff T, O'Driscoll M, Rief N, Iwabuchi K, Lobrich M, Jeggo PA (2004) ATM and DNA-PK function redundantly to phosphorylate H2AX after exposure to ionizing radiation. *Cancer Res* **64:** 2390–2396

Stiff T, Walker SA, Cerosaletti K, Goodarzi AA, Petermann E, Concannon P, O'Driscoll M, Jeggo PA (2006) ATR-dependent phosphorylation and activation of ATM in response to UV treatment or replication fork stalling. *EMBO J* **25:** 5775–5782

Tian B, Yang Q, Mao Z (2009) Phosphorylation of ATM by Cdk5 mediates DNA damage signalling and regulates neuronal death. *Nat Cell Biol* **11:** 211–218